

Deposition of Nanocrystalline-Silicon by Cat-CVD Method and its Characterization

S. Godavarthi^{1,2}, Y. Matsumoto¹, V. Subramaniam¹ and P. S. Mallick²

¹Electrical Engineering Department, Centro de Investigación y de Estudios Avanzados del IPN, Av. IPN 2508 Col. San Pedro Zacatenco, Mexico City 07360, México, Tel: 55-5747-3783, e-mail: ymatsumo@cinvestav.mx

²School of Electrical Sciences, Center for Nanotechnology, VIT University, Vellore, India

Abstract — Silicon and its related alloys deposited by catalytic chemical vapor deposition (Cat-CVD), takes place upon thermo-catalytic decomposition of the reactant gases, i.e. silane (SiH₄) and hydrogen (H₂), at the surface of a hot filament. Tantalum (Ta) has been used as catalyst which resulted with better controllability from amorphous to crystalline-phase transition.

Process for depositing hydrogenated nanocrystalline silicon (nc-Si:H) embedded in hydrogenated amorphous silicon oxide (a-Si:O:H) matrix, as a function of both, Ta-catalyst, and substrate-temperatures are reported. The deposited samples were characterized by X-ray diffraction and micro-Raman spectroscopy. Crystalline sizes were determined using a Sherrer's formula and Raman spectra for its size-related tendencies. As preliminary results, the range of crystallite formation starts at the catalyst temperature of 1700 ~ 1750 °C.

Keywords — Nanocrystalline-silicon, Cat-CVD, X-ray-diffraction, micro-Raman

I. INTRODUCTION

It is undeniable fact that Silicon (Si), is the most important material in the semiconductor world dominating in integrated circuits, memories, sensors and more recently, for solar cell mass production. This is because of advantages as stable and strong material with same crystal structure as diamond. On the other hand, excellent oxide forms with Si; the interface has a very low-state density. Up until now, different types of thin film silicon materials have been developed for several applications: amorphous-Si:H [1] (a-Si:H), protocrystalline [2] (pr-Si:H), polymorphous [3] (pm-Si:H), nanocrystalline [4] (nc-Si:H), microcrystalline [5] (μ c-Si:H) and polycrystalline silicon [6] (poly-Si:H). In all cases, the H in the abbreviation stands for hydrogenated, due to the presence of this element in the silicon network. At first sight, the different morphologies could be generally classified by the differences in the amount of amorphous phase present and the crystallite size.

Many nc-Si is referred to a two-phase amorphous and crystalline material with grain sizes of the order of tens of nm. Throughout this work, the term employed to describe the above-mentioned material will be nc-Si:H.

The term nanocrystalline silicon refers to a range of materials around the transition region from amorphous to microcrystalline phase in the silicon thin film.

A great number of techniques can be used to produce nc-Si embedded in a-Si:H, such as sputtering [7-10], ion implantation [11-13] plasma enhanced chemical vapor deposition (PE-CVD) [14,15], low-pressure CVD (LPCVD) [16], pulsed laser deposition (PLD) [17, 18],

Catalytic-CVD (Cat-CVD) [19]. It was shown that variation of the parameters of nc-Si creation processes allows controlling the light emitting properties.

In this work, the nanocrystalline silicon (nc-Si) embedded in hydrogenated amorphous silicon oxide (a-Si:O:H) matrix is reported. Structural and bonding properties as a function of filament temperature, substrate temperature and hydrogen flow will be discussed.

The deposited films were characterized with X-ray diffraction (XRD) and micro-Raman spectroscopy (MRS) to determine crystallites size tendencies.

II. EXPERIMENTAL

A. Deposition of nanocrystalline-Si

The Cat-CVD system has been already described elsewhere [20]. The reaction chamber as well as reaction at the catalyst is shown in the Fig 1. Reaction chamber houses the gas outlet, catalyst, shutter, substrate-holder, and an optical window for filament temperature measurement which is monitored by an IR detector (Chino model IR-AHS).

Source gases were introduced into the reaction chamber through a 1/8" stainless steel tube. The gas flow is controlled by mass flow controller (model MKS). This mass flow controller arrangement should be in specified directions.

The chamber pressure was settled and automatically controlled by means of electro-mechanic throttle valve. The distance between the catalyst and sample, and also between the gas tubing and catalyst, was settled to 5 cm.

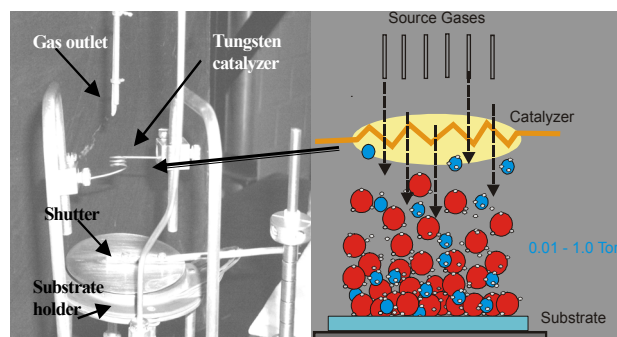


Fig. 1. Internal description of the reaction chamber. Consist in components as source gases outlet, filament (catalyst), shutter and substrate holder. The schematic reaction at the catalyst is also shown at the right side.

Films were deposited on glass substrates simultaneously on crystalline silicon (c-Si) substrates. The glass substrates were Corning 3070 of 1.1mm thickness and c-Si are one-side mirror polished boron-doped P-type and of 525 μm thickness.

The c-Si and glass substrates have been cleaned from organic and inorganic impurities by using the conventional RCA method.

The gases used for deposition of films were SiH_4 , O_2 and H_2 . The flow rates of SiH_4 and O_2 were kept constant at 5 Standard Cubic Centimeter per Minute (sccm), and the deposition time was also kept constant for 20 minutes.

The depositions carried at different catalyst temperatures (T_{fil}), substrate temperatures (T_{sub}) and H_2 flow parameters. The T_{fil} varied 1700 to 1950°C in steps of 50°C. The T_{sub} changed from 150 to 250°C in steps 50°C and controlled by the Hydrogen flow rate changed from 5 to 20 sccm in steps of 5 sccm. The list of the sample conditions which were deposited during this work is given in the Table I.

III. CHARACTERIZATION

X-ray diffraction spectroscopy

The deposited films were analyzed by X-ray diffraction (XRD) using Siemens D5000 at a galancing angle of 2° . These patterns were employed to analyze the orientation as well as crystallite size of the nc-Si samples, based on Scherrer's formula [21].

The crystallite Size was determined as $X_{\text{size}} = 0.89 * \lambda / \text{FW} * \cos \theta$; where λ (1.54056Å) is the XRD wavelength, θ is the peak position and FW (in radians) is the full width at half maximum (FWHM) intensity of the diffraction peaks.

Figures 2 to 6 shows XRD patterns of deposited samples. Three main peaks are observed in several samples. The peak at 28.4° , 47.3° and 56.1° are corresponding to the Si (111), (220) and (311) planes, respectively. One more peak is observed in a few samples, mostly at filament temperatures above 1800°C, at 25.6° belongs possibly to SiO_x -related phase. The broad area under the Si (111) peak could be due to the glass substrate component indicates its amorphous phase.

A. The role of catalyst temperature

Fig. 2. shows the nc-Si tendency with increasing catalyst temperature (bottom to top) at $T_{\text{sub}} = 200^\circ\text{C}$ and $\text{SiH}_4/\text{O}_2/\text{H}_2=5/5/10$.

For the sample prepared at $T_{\text{fil}} = 1750^\circ\text{C}$, the (111) crystalline plane is the preferential orientation which shows a clearer peak. One of the possible reason could be its thickness dependence for the samples. The deposited sample thicknesses are ranging from 200-400 nm, which is different from reported [22, 23] having thickness of one micron or above. Glass substrate may also contribute to some preferential crystalline-phase growth depending of deposition conditions. The size tendency with respect to filament temperature, substrate temperature and hydrogen

TABLE I

The list of the deposited samples with the corresponding hydrogen flow in sccm. (Source gases were fixed to: $\text{SiH}_4/\text{O}_2=5/5$) the acronym "a" and "c" denotes the film structure observed by XRD as amorphous or crystallite phases, respectively

$T_{\text{sub}} (^\circ\text{C}) \backslash T_{\text{fil}} (^\circ\text{C})$	150	200	250
1700	5a 15a	5a 10a 15a 20a	5a 15c
1750	5a 10c	5c 10c 15c 20c	5c 10c 15c 20c
1800	5c 10c 15c 20c	5c 10c 15c	
1850	10c	5c 10c 15c	10c
1900		5c 10c 15c	

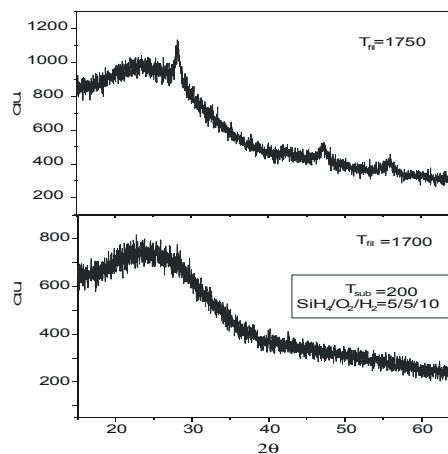


Fig. 2. XRD spectra for sample prepared at different catalyst temperature with: $T_{\text{sub}} = 200^\circ\text{C}$ and $\text{SiH}_4/\text{O}_2/\text{H}_2=5/5/10$.

flow is explained in following sections.

In Cat-CVD, the heated catalyst mainly decomposes SiH_4 into Si and H. These products easily react in gas phase giving as a result different radical species depending on the process pressure and the catalyst to substrate distance. The dissociation mainly depends on filament temperature. As from Fig. 2, it is noted that as a function of the catalyst temperature increment, it appears the crystal-like peaks for corresponding silicon characteristic.

TABLE II

Crystallite size variation as a function of the catalyst temperature.

(SiH₄/O₂/H₂= 5/5/15), T_{sub}=200°C, see Fig. 3.

Catalyst Temp.	(111) (nm)	(220) (nm)	(311) (nm)	Average (nm)
1850 °C	19.8	8.6	12.7	13.7
1800 °C	13.8	6.1	6.8	8.9
1750 °C	15.3	7.7	-	7.6
1700 °C	-	-	-	-

Fig. 3. shows also nc-Si formation tendency with increasing the catalyst temperature (bottom to top) for T_{sub} = 200°C and SiH₄/O₂/H₂=5/5/15. The corresponding preferential orientations and average crystallite sizes are given in the Table II. From Fig. 3 and Table II, no crystallite formations are apparent at T_{fil}= 1700°C i.e. film remains in amorphous phase. However, the crystallites starts growing at T_{fil} = 1750°C and the size of crystallite seems to increases with increasing catalyst temperature. In the samples presented, the observed results could be related due to the differences in the dissociated amount of SiH₄ and its energy at the catalyst. The mole fraction of SiH₄ not being decomposed by a tantalum catalyst decreases with increasing T_{fil} [24]. This means that at lower T_{fil}, there is more SiH₄ left for being consumed in the reaction SiH₄+H-SiH₃+H₂ and, therefore, that less SiH₃ radicals are produced at relatively low temperature. This radical is considered to be main precursor for the growth of quality a-Si:H in PECVD and is likely to provoke that material grown in the adequate conditions. Additionally, for samples deposited at the catalyst temperature from 1800°C, independently of the hydrogen flow or substrate temperatures, in the obtained film always appear crystalline phases. (see Table I).

B. The role of substrate temperature

Fig. 4 shows the XRD spectra for samples prepared at different substrate temperatures at fixed T_{fil} = 1700°C and SiH₄/O₂/H₂=5/5/15. The deposited films are in amorphous phase for samples prepared at T_{sub} = 200°C and below, i.e no crystallites are formed when the catalyst temperature of 1700°C. At T_{sub} = 250°C, the crystallites starts growing and found that the average size is below 10nm.

The substrate temperature effect could be explained as follow. At low substrate temperatures, deposited atoms, molecules or radicals are not in positions to diffuse and to accommodate themselves to form a crystalline-involved structure, since they have low energy. However, with increasing the substrate temperature, the energy possessing by these radicals will increase. They can diffuse on the surface so that they can accommodate themselves to form crystalline.

The substrate temperature plays definitely an important role for crystallite formation. In comparison to the Fig. 4, Fig. 5 shows XRD spectra for the samples deposited at the same range of substrate temperature as Fig. 4, but at the

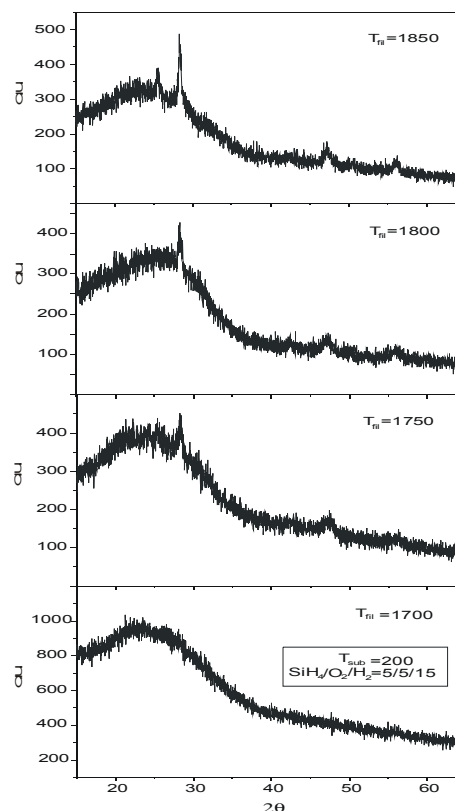


Fig. 3. XRD spectra for sample prepared at different catalyst temperatures with: T_{sub}=200°C and SiH₄/O₂/H₂=5/5/15.

catalyst temperature of 1750°C.

As compared to samples prepared in Fig. 4, in spite of lower hydrogen flow of 5 sccm, the sample prepared at T_{sub} = 200°C starts promoting crystallite formation. From the previous results, the catalyst temperature has an important contribution for crystallite promotion.

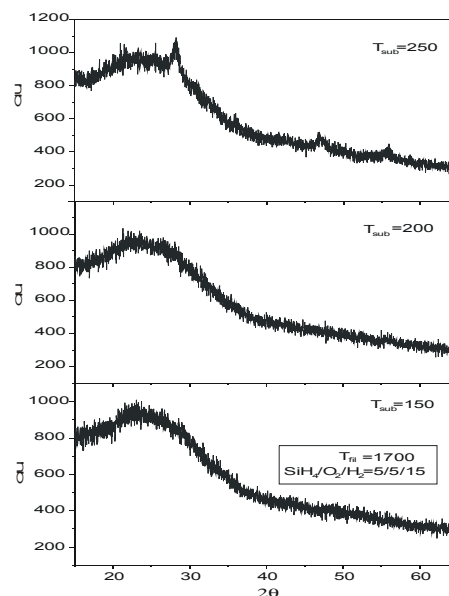


Fig. 4. XRD spectra for the samples deposited at different substrate temperatures with: T_{fil} = 1700°C and SiH₄/O₂/H₂=5/5/15.

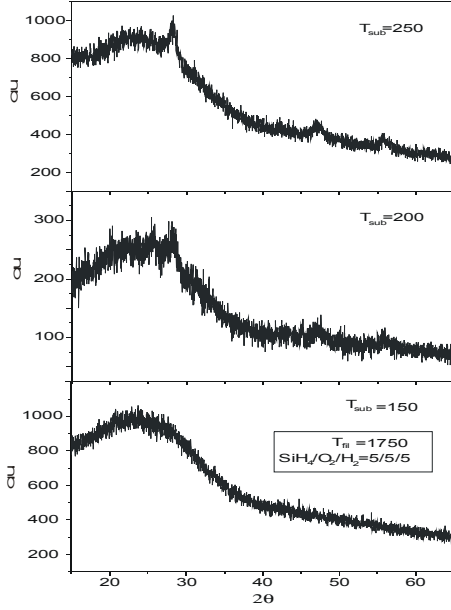


Fig. 5. XRD spectra for the samples deposited at different substrate temperatures, with: $T_{fil} = 1750^\circ\text{C}$ and $\text{SiH}_4/\text{O}_2/\text{H}_2 = 5/5/5$.

C. The role of hydrogen flow rate

With increasing H_2 dilution, the ratio radicals density changes which are assumed to play role in formation of nc-Si. So, it is also important to study the role of hydrogen in controlling the formation of nc-Si.

Fig. 6 shows the crystalline formation process as a function of hydrogen dilution, at $T_{fil} = 1700^\circ\text{C}$ and $T_{sub} = 250^\circ\text{C}$. It is observed that no crystallinity was observed at 5 sccm of hydrogen flow. However, at 15 sccm of hydrogen dilution, a formation of nanocrystallites was found. The average nanocrystallites size is around 8.7nm using Scherrer's formula.

At this moment, it is clear that hydrogen helps the crystallites formation by creating more Si-H radical species and/or atomic H^+ . The hydrogen-involved molecular decompositions may increase the diffusion length at the substrate surface. However, as is well known, H_2 flow rate increment decreases the deposition rate due to the etching process phenomena at the surface, i.e. the deposition speed is only slightly higher than that of the etching rate due to the H^+ . The etching effect avoids formation of weak-bonded molecules i.e. the formation of amorphous-phased dangling-bonds. Furthermore in the present case, the entire growth mechanism for the nc-Si material, has to be considered with the interaction of oxygen molecules, so the formation of a-Si:O:H. Conventionally the nc-Si nucleation occurs starting at the a-Si:H phases [25], but in the present circumstance, oxygen molecules acts also as Si-Si formation inhibitor.

Raman Spectroscopy

Raman Spectroscopy was used to determine nanocrystallites sizes. The spectrometer was Jobin-Yvon T64000 with He-Ne laser. The characteristic peak

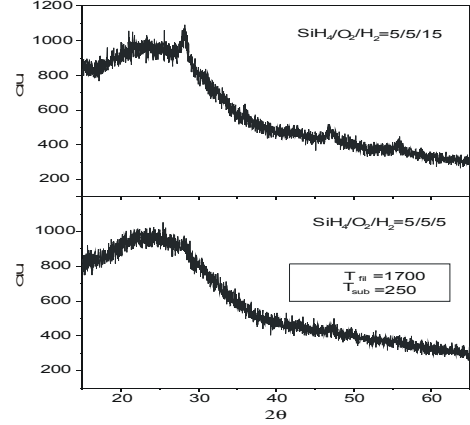


Fig. 6. XRD spectra for the samples deposited at different hydrogen flow at $T_{fil} = 1700^\circ\text{C}$ and $T_{sub} = 250^\circ\text{C}$, with constant flow for $\text{SiH}_4/\text{O}_2 = 5/5$.

corresponding to the transverse optical mode of crystalline silicon can be found at 520 cm^{-1} , whereas the amorphous band appears around 480 cm^{-1} .

The mean size of the nanocrystallites can be found using formula [26].

$$d = 2\pi \left(\frac{B}{\Delta\omega} \right)^{\frac{1}{2}} \quad (4.1)$$

Where d = size of the nanocrystallites,

$\Delta\omega$ = peak shift for the nanocrystalline as compared that of the c-Si
 $B = 2.0\text{ nm}^2\text{ cm}^{-1}$

The Raman spectra in Si, can be decomposed into two components: one is the crystalline phases that are responsible for the component at approximately 520 cm^{-1} and another is amorphous phase causing the component at approximately 480 cm^{-1} .

A. Raman for substrate temperature analysis

Fig. 7, shows the Raman spectra of the nc-Si films deposited at filament temperature 1750°C with different substrate temperatures which is corresponding to XRD spectra given in Fig. 5.

The films with substrate temperatures of 150°C exhibit Raman spectra peak at 480 cm^{-1} . But film with $T_{sub} = 200^\circ\text{C}$ and 250°C exhibited its peak at 518.02 cm^{-1} and 518.02 cm^{-1} , respectively showing the nc-Si phase (see Fig. 5). Substituting the peak shift in the above formula, it is observed that the deviation in the crystallite size is again observed in this case when compared with XRD.

It is known that Raman shifts are controlled by vibration of the electronic polarization for constituents in the films, which depend on the bonding structure such as atomic distance. Full width at half maximum (FWHM) in general broaden as the magnitude of the lattice strain which is widely distributed in a film. On the other hand, if the

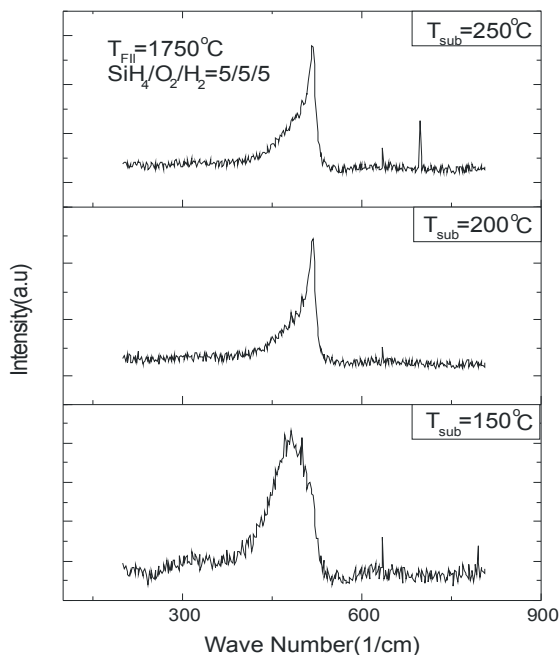


Fig. 7. Raman spectra for samples with different T_{sub} at $T_{\text{fil}}=1750^{\circ}\text{C}$ and $\text{SiH}_4/\text{O}_2/\text{H}_2=5/5/5$

atomic distance uniformly strained, the width of the Raman spectrum will be unchanged, but its peak frequency should shift. So blue shift may result due to strain in the film and results low crystallite size.

V. CONCLUSION

nc-Si: H embedded in a- Si:O:H films are deposited using Ta catalyst in Cat-CVD process. The deposited samples are characterized by XRD and Raman spectroscopy for determination of size of the nc-Si.

nc-Si is observed at T_{fil} as low as 1700°C , however, the lowest crystallite size of 7.6 nm was found at $T_{\text{fil}}=1750^{\circ}\text{C}$; $T_{\text{sub}} = 200^{\circ}\text{C}$ and $\text{SiH}_4/\text{O}_2/\text{H}_2 = 5/5/15$.

The formation and the variation of nc-Si size with different parameters such as filament temperature, substrate temperature and hydrogen flow rate was discussed. It is observed that the crystallite size is easily growing with increase of catalyst temperature and with a fixed T_{sub} and H_2 flow rate.

It is observed that at $T_{\text{fil}}=1750^{\circ}\text{C}$ and above the crystallite size grows with increase of T_{sub} with irrespective of H_2 flow rate. Some reason was assumed by considering the PECVD case.

It is observed that increasing the H_2 flow, decreases the deposition rate. This in turn results in depositing-etching effect of Si-H-Si network which is important in the formation of nc-Si. However, it is supposed that size of the nc-Si depends on H_2 flow rate as well as Si-Si network formation rate involving oxygen molecules.

The values of nc-Si size measured from Raman spectra are deviating from the XRD values. This was explained by considering possibly the strain present in the film.

ACKNOWLEDGMENT

The authors thank Angela Gabriela López for sample preparations. The authors are indebted to Miguel Angel Luna for sample thickness measurements, Marcela Guerrero and Alejandra García of Physics Department for XRD and Raman measurements, respectively.

REFERENCES

- [1] H. Shanks, C. J. Fang, L. Ley, M. Cardona, F. J. Demond, S. Kalbitzer., *Physica Status Solidi (b)* 100 (1980) 43.
- [2] J. Koh, A. S. Ferlauto, P. I. Rovira, C. R. Wronski and R. W. Collins, *Appl. Phys Lett* 75 (1999) 2286.
- [3] A. Fontcuberta, H. Hfmeister and P. Roca I Cabarrocas, *Jouranal of non-crystalline solids* 299-302 (2002) 284-289.
- [4] Nobuyasu Suzuki, Toshiharu Makino, Yuka Yamada, and Takehito Yoshida, *Applied Physics Letters*, 76 (2000) 1389.
- [5] J. Meier et al, *Solar Energy Materials and solar cells*, 49 (1997) 35.
- [6] R.E.I. Schropp and J.K. Rath, "Novel Profiled Thin Film Polycrystalline Silicon Solar Cells on Stainless Steel Substrates", Special issue *IEEE Transaction on Electron Devices*, on Progress and Opportunities in Photovoltaic Solar Cells Science & Engineering, *IEEE Trans. Electron Dev.* 46, No. 10 (1999) 2069-2071.
- [7] Y. Kanzawa, T. kageyama, S. Takeoka, M. Fujii, S.Hayashi, K.Yamamoto, *Solid State Commun*, 02 (1997) 533.
- [8] L.Tsybeskov, K.D Hirschman, S.P. duttagupta, M.Zacharias, P.M. Fauchet, J.P. McCafey, D.J. Lockwood, *Appl. Phys. Lett.* 72 (1998) 43.
- [9] S.Charvet, R.Madelon, R. Rizk, *solid State Electron.* 45 (2001) 1505.
- [10] T.V. Torchynska, M.M. Rodriguez, Y. Golstein, A. Many, E. Endzewski, B.M. Bulakh, L.V. Scherbina, *Physica B* 308-310 (2001) 948.
- [11] B. Garrido, M. Lopez, S. Ferre, A. Romato-Rodriguez, A. Perez-Rodriguez, P. Ruterana,, J.R Morante, *Nucl. Instrum. Meth. B* 120 (1996) 101.
- [12] H.Z song, X.M Bao, *Phys. Rev. B* 55 (997) 6988.
- [13] S.Chelan, R.G. Elliman, *Appl. Phys. Lett.* 78 (2001) 1912.
- [14] G. Franzo, F. Iacona, C. Spinella, S. Cammarata, M.G. Grimaldi, *Mater. Sci. Engng B* 69/70 (2002) 454.
- [15] T. Inokuma, Y. Wakayama, T. Muramoto, R. Aoki, Y. Kurata, S. Hasegawa, *J. Appl. Phys.* 83 (1998) 2228.
- [16] A. Morales, J. Barreto, C. Dominguez, M. Riera, M. Aceves, J.Carrillo, *Physica E* 38 (2007) 54-58.
- [17] Jong Hoon Kim, Kyung Ah Jeon, Gun Hee Kim, Sang Yeol Lee, *Optical Materials* 27 (2005) 991-994.
- [18] Nobuyasu Suzuki, Toshiharu Makino, Yuka Yamda, and Takehito Yoshida, *Applied Physics Letters*, 76(11) (2000) 1389 .
- [19] T.V. Torchynska, A.Vivas Hernandez, M.Dybiec, Yu.Emirov, I.Tarasov, S.Ostapenko and Yasuhiro Matsumoto, *Phys. Stat. Sol.* 2, N° 6, (2005) 1832-1836.
- [20] Y.Matsumoto., *Thin Solid Films* vol 501, (2006) 95-97.
- [21] B.D. Cullity., 2nd ed., (Addison- Wesley, Reading, MA, 1978) 284-285
- [22] J. Cifre, J. Betimeu, J. Puigdollers, M. C. Polo, J. Andresu, A. Lloretm, *Appl. Phys.* A59 (1994) 645.
- [23] M. Fonrodona, D.Soler, J.m Asensi, J. Bertomeu, J. Andreu, J. Non-Cryst. Solids 299-302 (2002) 14-19.
- [24] A. Pant, T. W. F. Russell, M. Huff, R. Aparicio, R.B. Birkmire, *Ind. Eng. Chem. Res* 40 (2001) 1377.
- [25] H. Fujiwara, M. Kondo, A. Matsuda, *Jpn. J. Appl. Phys.* 41(2002) 2821.
- [26] Yuilang He , Chenzhong Yin, Guangxuxu cheng, Luchun Wang, and xiangna Liu., *J. Appl. Phys.* 75 (2) (1994) 797.